International Journal of Engineering Science 105 (2016) 108–127

Contents lists available at ScienceDirect

International Journal of Engineering Science

journal homepage: www.elsevier.com/locate/ijengsci

Determination of pressure data from velocity data with a view toward its application in cardiovascular mechanics. Part 1. Theoretical considerations

H. Švihlová [a], J. Hron [a], J. Málek [a], K.R. Rajagopal [b,*], K. Rajagopal [c]

[a] Charles University in Prague, Faculty of Mathematics and Physics, Mathematical Institute, Sokolovská 83, 186 75 Prague, Czech Republic
[b] Texas A&M University, Department of Mechanical Engineering, College Station, TX 77843-3132, United States
[c] Center for Advanced Heart Failure and Department of Cardiothoracic/Vascular Surgery, University of Texas-Houston and Memorial Hermann Texas Medical Center 6400 Fannin, Suite 2350, Houston, TX 77030, USA

ARTICLE INFO

Article history:
Received 25 October 2015
Revised 20 November 2015
Accepted 21 November 2015
Available online 29 January 2016

Keywords:
Non-invasive pressure determination
Pressure-Poisson equation
Stokes equation
Heart valve
Blood vessel

ABSTRACT

The non-invasive determination of the pressure (mean normal stress) in a flowing fluid has ramifications in a variety of important problems: the flow of blood in blood vessels, flows taking place in inaccessible locations in complex internal geometries that occur in mechanical systems, etc. In this paper we discuss a rigorous new mathematical procedure for the determination of the pressure (mean normal stress) field, from data for the velocity field that can be obtained through imaging procedures such as 4D magnetic resonance imaging or echocardiography. We then use the procedure to demonstrate its efficacy by considering flows in an idealized geometry with a symmetric and asymmetric obstruction. We delineate the superiority of the method with regard to the methods that are currently in place. In Part 2 of this two part paper, we study the loss of pressure and the dissipation that occurs due to the flow of blood across a diseased valve (the pressure loss being an important indicator of the extent of the valvular disease) as well as the flow taking place in a realistic cerebral aneurysm.

1. Introduction

The ability to non-invasively determine the pressure in a flowing fluid has wide ranging technological relevance and import, an example being problems in medicine concerning the flow of biological fluids. The cardiovascular system presents several situations wherein the non-invasive determination of pressure would significantly reduce serious risks associated with invasive procedures. This two part study is concerned with the determination of the pressure field from non-invasive velocity data with a view toward determining the pressure drop across a diseased valve as a consequence of the dissipation in the fluid as it flows through the valve, the loss of pressure bearing a direct relation to the extent of the disease. While there have been some careful mathematical attempts at determining the pressure field from information for the velocity field, with regard to the Navier–Stokes fluid (see the references below), most of the studies concerning the determination of pressure from the velocity data with regard to flow across diseased valves and other related cardiovascular flow problems are based on an appeal to inappropriate governing equations, namely the Bernoulli equation, which are grossly inadequate to describe the dissipation that takes place in a flowing fluid. This is usually addressed by an ad hoc modification to the Bernoulli equation by adding a dissipation term; see

* Corresponding author. Tel.: +1 9798200782.
E-mail addresses: helena.svihlova@seznam.cz (H. Švihlová), jaroslav.hron@mff.cuni.cz (J. Hron), josef.malek@mff.cuni.cz (J. Málek), krajagopal@tamu.edu (K.R. Rajagopal), keshava.rajagopal@uth.tmc.edu (K. Rajagopal).

http://dx.doi.org/10.1016/j.ijengsci.2015.11.002
0020-7225/

Akins, Travis, and Yoganathan (2008). What is however required is a much more careful consideration of the viscous dissipation that takes place during the fluid flow and the resulting pressure drop. We discuss in detail the inverse problem of determining the pressure field from data for the velocity field which might or might not be known precisely. The study does not appeal to the Bernoulli equation but considers in full the Navier–Stokes equations for an incompressible linearly viscous fluid. In Part 1 of the study, in order to clarify and simplify the procedure, we consider the flow in an idealized geometry of the stenotic aortic valve. In Part 2 we will present a broader study concerned with determining the dissipation directly from the model. Part 2 will include results concerning the extent of dissipation and the corresponding pressure drop, in geometries with different levels of the severity (up to 85% in symmetric stenotic valves) and we also present some results concerning the determination of pressure in flows occurring in cerebral aneurysms in realistic geometries. In Part 1, we provide the details of the mathematical issues and the numerical procedures that are adopted to obtain the pressure field from the velocity field, while the motivation for the consideration of the problem of Valvular stenosis and Valvular disease is provided in Part 2.

While blood in small vessels exhibits shear-thinning characteristics, in a vessel of the size under consideration it can be modeled as a Navier–Stokes fluid. The resulting equations for the pressure determination can be expressed in two different ways, one as a Poisson equation for the pressure field and the other based on the Stokes equation with additional stabilization/correction term. The former method even in the weak form requires higher derivatives than the latter method. In order to ascertain the efficiency of the two methods we compute the pressure field corresponding to three types of velocity data, the first which we refer to as "fine data" wherein we have full information for the velocity field on a very fine grid, the second type of data which we refer to as "coarse data" wherein the information is available only on a rough grid with a different level of coarseness, and finally the third type of data, "data with a noise", wherein the first two types of data are combined with an uncertainty in its values. We compare the results for the pressure field obtained from the three types of data for the velocity field using the two different methods, the pressure Poisson equation (PPE) method and the Stokes equation (STE) method. To our knowledge such a comparative study of the numerical schemes that delineates the differences in the results from the two schemes and which clearly indicates the STE method to be superior to the PPE method, for the problem on hand, have not been carried out.

We idealize the geometry of the flow to a flow in a rigid pipe with an obstruction knowing full well that the real flow domain is far more complicated with the walls being highly deformable. Our aim is to solve eventually such a complex problem for the determination of the pressure field from the data for the velocity field. While we have some experience in the numerical resolution of problems concerning fluid–solid interactions with regard to a direct determination of the velocity and pressure fields, see Hron and Madlik (2007), Razzaq, Damanik, Hron, Ouazzi, and Turek (2012), we have to develop the codes in the case of the problem of determining the pressure field from a knowledge of the velocity field. In Part 2 of the paper we consider the flow in the actual geometry that matches anatomical conditions. In this Part 1, our aim is to establish the proof of concept with regard to the mathematical formulation and the numerical procedure. We do use physiologic data for the inlet and outlet condition upstream and downstream of the obstruction (stenosis) but the flow geometry is idealized.

1.1. Determining the pressure for the flow of the Navier–Stokes fluid

The pressure loss across a diseased valve or stenotic artery is thought to be due to the dissipation that takes place during the flow across the valve. In view of this, there has been a great deal of effort expended in determining the dissipation due to the flow across a diseased valve; see Akins et al. (2008) and Dasi, Simon, Sucosky, and Yoganathan (2009). However, all these efforts are totally ad hoc and appeal to procedures that are clearly not suited for evaluating the dissipation. This is because the approaches used to non-invasively ascertain energetic losses are arbitrary modifications of models that actually describe conservation of energy; the very essence of a stenosis is that it poses an impedance to flow, dissipating the energy of flowing blood. The walls of the blood vessel are in fact inhomogeneous and anisotropic, and more importantly viscoelastic. Thus, in order to determine the flow characteristic of blood across a diseased valve, it is necessary to solve the equations that couple the motion of the wall boundary as well as the equations governing the flowing blood. The problem is exceedingly difficult in view of the fact that the flow domain is changing with time and the domain itself can only be determined by solving the coupled system of equations. It is our aim to eventually study such a problem. Here we study flows in a geometry with rigid boundaries.

In very small blood vessels such as capillaries as the diameter of the red blood cells are of comparable or even larger diameter than that of the blood vessel, even using a continuum fluid model for blood is totally inappropriate. However, in the problem of flow across a diseased valve or arterial stenosis the flow of blood can be well described by the classical incompressible Navier–Stokes fluid. Even if we consider the fluid flowing in a vessel that has a rigid boundary, the problem is quite challenging as we have to solve the problem wherein locally the Reynolds number is very large, the geometry of the flow domain is complex, and the flow is three dimensional and unsteady.

Let us suppose that blood can be described by the Navier–Stokes constitutive relation, that is

$$\mathbf{T} = -p\mathbf{I} + 2\mu\mathbf{D}, \tag{1}$$

where $\mathbf{T}$ is the Cauchy stress, $p = -\frac{1}{3}(\operatorname{tr}\mathbf{T})$ is the mean normal stress that is usually referred to as the mechanical pressure (see Rajagopal, 2015 for a detailed discussion of the notion of "pressure"), μ is the dynamic viscosity, $\mathbf{v}$ is the velocity and $\mathbf{D} = \frac{1}{2}\left(\nabla\mathbf{v} + \left(\nabla\mathbf{v}\right)^T\right)$. Since the fluid is incompressible, it can only undergo isochoric motions so that the constraint

$$\operatorname{tr}\mathbf{D} = \operatorname{div}\mathbf{v} = 0 \tag{2}$$

is satisfied. We shall assume that the fluid is homogeneous and hence the balance of mass reduces to the density ϱ being a constant everywhere.

On neglecting body forces and substituting the constitutive relation (1) into the balance of linear momentum

$$\varrho \frac{\mathrm{d}\mathbf{v}}{\mathrm{d}t} = \operatorname{div} \mathbf{T}, \tag{3}$$

where ϱ is the density, and $\frac{\mathrm{d}}{\mathrm{d}t}$ is the material time derivative given by

$$\frac{\mathrm{d}\mathbf{v}}{\mathrm{d}t} = \frac{\partial \mathbf{v}}{\partial t} + (\nabla \mathbf{v})\mathbf{v}, \tag{4}$$

and on dividing by the constant ϱ we obtain the Navier–Stokes equation for an incompressible fluid, namely

$$\frac{\partial \mathbf{v}}{\partial t} + (\nabla \mathbf{v})\mathbf{v} + \nabla \frac{p}{\varrho} - \operatorname{div}(2\nu \mathbf{D}(\mathbf{v})) = 0 \qquad \forall (\mathbf{x}, t) \in \Omega \times \mathcal{R} \tag{5}$$

with kinematic viscosity $\nu = \frac{\mu}{\varrho}$.

Now instead of trying to get some sort of an estimate on the loss of pressure as a consequence of the dissipation, we discuss in Section 1.1 how to directly obtain the pressure field once the velocity field is known. The velocity field is assumed to have been determined by either echocardiography or 4D magnetic resonance imaging, and we will consider both knowledge of the velocity field at a limited number of the points and the possibility of uncertainty of the values for the velocity field.

In general one would like to find a solution to the Navier–Stokes systems (5) and (2), with velocity as close as possible to the available velocity measurement. However, let us initially assume we know the velocity field possibly satisfying (2) and we look for the pressure p such that the pair $(\mathbf{v}, p)$ solves also (5). In biomedical context this has been investigated for example in Heys et al. (2010), Gurka, Liberzon, Hefetz, and Rubinstein (1999), Yang, Kilner, Wood, Underwood, and Firmin (1996), Krittian et al. (2012), Bolin and Raguin (2008), Charonko, King, Smith, and Vlachos (2010), Song, Leahy, Boyd, Brundage, and Napel (1994), and Dabiri, Bose, Gemmell, Colin, and Costello (2014). See also Van Oudheusden (2013) for an overview of other areas than biofluid mechanics where the problem of pressure recovery from measured velocity data is investigated.

In all of the cited references, the PPE method is used to compute the pressure. We compare the PPE method, as described in Section 1.1.1, with a new approach, namely the STE method as presented in Section 1.1.2. The STE method is based on the Helmholtz decomposition theorem (see for example Maria Denaro, 2003 for its application in the context of projection methods), and it allows us to compute the pressure under lower regularity requirements on the given velocity. In Cayco and Nicolaides (1986), this approach is used to recover pressure for two-dimensional flows that allows the authors to use the stream function formulation. However we have not found any publication using this method to recover the pressure for a given velocity field in general three dimensional flows. In Section 2 we show that the STE method provides more accurate pressure approximation than the PPE method for the same velocity data. Of course, in the STE method we solve a system of four partial differential equations in three dimensions, while the PPE method requires solving just one scalar equation.

In general one can try to solve a constrained optimization problem of the type: find the couple $(\mathbf{w}, q)$ such that it satisfies the Navier–Stokes equation inside the domain Ω while simultaneously the velocity field $\mathbf{w}$ is close to the measured velocity $\mathbf{v}$ in some sense. This has been considered for example in Heys et al. (2010) where the Galerkin least squares method (GLS) is used to recover the pressure from Particle Image Velocimetry measurements. In this case, there is no need to compute any derivatives of the given (i.e. measured) velocity field. On the other hand one has to solve a symmetric, positive definite, much larger nonlinear system of equations. In this study we will restrict ourselves to linear methods.

1.1.1. Determination of the pressure by the PPE method

We now start with a discussion of the PPE method. We can derive from (5), for $q_{\mathrm{ppe}} \approx p$, that

$$-\nabla q_{\mathrm{ppe}} = \mathbf{f}(\mathbf{v}), \tag{6}$$

where we define the quantity

$$\mathbf{f}(\mathbf{v}) = \varrho \frac{\partial \mathbf{v}}{\partial t} + \varrho (\nabla \mathbf{v})\mathbf{v} - \operatorname{div}(2\mu \mathbf{D}(\mathbf{v})) \tag{7}$$

which depends only on the given velocity field $\mathbf{v}$.

On taking the divergence of the Navier–Stokes equations (5) we obtain, in virtue of the incompressibility condition (2), that

$$-\Delta p = \varrho \nabla \mathbf{v} \cdot (\nabla \mathbf{v})^T. \tag{8}$$

Since the real problem takes place in a complex geometry, we will have to solve Laplace's equation (8) numerically. For a given velocity field $\mathbf{v}$, which may not be necessarily divergence free and consequently $\operatorname{div} \mathbf{f}(\mathbf{v})$ differs from the right hand side of (8), we want to solve the problem for $q_{\mathrm{ppe}} \approx p$, where q_{ppe} meets

$$-\Delta q_{\mathrm{ppe}} = \operatorname{div} \mathbf{f}(\mathbf{v}), \tag{9}$$

$$\frac{\partial q_{\mathrm{ppe}}}{\partial \mathbf{n}} = -\mathbf{f}(\mathbf{v}) \cdot \mathbf{n} \tag{10}$$

with $\mathbf{f}(\mathbf{v})$ given by (7). We approximate $\frac{\partial \mathbf{v}}{\partial t}$ in (7) by $\frac{\mathbf{v}-\mathbf{v}^k}{t^{k+1}-t^k}$ where $\mathbf{v}$ is a given velocity field at the current time step t^{k+1} and $\mathbf{v}^k$ is (also given) the velocity field at previous time step t^k.

Table 1
Relative errors for fine data.

	$\frac{\|q_{ppe}-p_{ref}\|_{L^2}}{\|p_{ref}\|_{L^2}}$	$\frac{\|q_{ste}-p_{ref}\|_{L^2}}{\|p_{ref}\|_{L^2}}$
Symmetric	6.40e−04	1.50e−14
Non-symmetric	3.50e−03	1.16e−14

Since this problem admits a unique solution up to a constant we need to supply some additional condition to have a uniquely defined solution. We will provide information of the mean value of the pressure over the outlet of the domain to determine the unique solution.

We refer to the problem of finding a numerical solution of (9) and (10) with (7) and this additional condition fixing the value of pressure as the PPE method.

This method is described for example in Heys et al. (2010), Gurka et al. (1999), Yang et al. (1996), Krittian et al. (2012), Bolin and Raguin (2008), Charonko et al. (2010), Song et al. (1994), Dabiri et al. (2014), and Shirokoff and Rosales (2011) and is closely connected to a projection step in the projection methods used to decouple the velocity–pressure computation when solving the Navier–Stokes equations, see for example Liu, Liu, and Pego (2010), Prohl (2008), and Guermond, Minev, and Shen (2006). In Song et al. (1994) it is shown that the PPE method is equivalent to finding a pressure p such that the functional $||\nabla p + \mathbf{f}(\mathbf{v})||^2_\Omega$ is minimized.

Eq. (9) is a second order partial differential equation. In order to solve (9) for p, we need to know the appropriate boundary conditions for p. Boundary conditions are determined by the physics of the problem. However, when one is unable to determine the appropriate boundary conditions based on an understanding of the physics of the problem, one can take recourse to a mathematical procedure that is reasonable and expected of the solution to the problem, provided one is assured of a solution that is sufficiently smooth. One can obtain conditions by evaluating the governing partial differential equation on the boundary.

This method leads to a scalar linear problem. However even in the weak form it requires computation of first or even second derivatives of the velocity field, depending on how many derivatives we can move to the test functions, which can be problematic if the velocity field is measured.

1.1.2. Determination of the pressure using the STE method

In this approach, based on the idea that stems from Cayco and Nicolaides (1986), we want to directly determine pressure as a function q_{ste} such that $-\nabla q_{ste} = (\mathbf{v})$ in a weak sense, where $\mathbf{f}(\mathbf{v})$ is given by (7).

This is done by solving a Stokes problem for the unknowns $\mathbf{w}$ and $q_{ste} \approx p$ such that

$$-\Delta \mathbf{w} - \nabla q_{ste} = \mathbf{f}(\mathbf{v}) \qquad \text{in } \Omega, \tag{11}$$

$$\operatorname{div} \mathbf{w} = 0 \qquad \text{in } \Omega, \tag{12}$$

$$\mathbf{w} = \mathbf{0} \qquad \text{on } \Gamma. \tag{13}$$

It is important to recognize that $\mathbf{w}$ is considered here as an unknown and has nothing in common with the given velocity $\mathbf{v}$. In fact, $\mathbf{w}$ is expected to be almost zero. Again we need to have a priori knowledge of the pressure at one point, or the mean value of the pressure over some part of the domain or its boundary, to get a unique solution.

The solution of (11)–(13) with the right hand side of (7) and the prescribed mean pressure value over the outlet is referred to as the STE method.

This method leads to a larger linear saddle-point type system of equations. However it requires less regularity on the data than the PPE method introduced in the previous section since no additional derivative of the data vector $\mathbf{f}(\mathbf{v})$ is needed.

1.1.3. Weak formulation of the problems

The subsequent computations are run using the automated finite element solver (Logg, Mardal, & Wells, 2012) which allows for an easy employment of the standard finite element method to a wide class of variational problems. First, the Navier–Stokes problem (5) and (2) is written in variational form as:

Find $(\mathbf{v};\, p) \in \{\mathbf{v}_D + V\} \times P, V = \{\mathbf{v} = (\mathbf{v}_1, \mathbf{v}_2, \mathbf{v}_3);\ \mathbf{v}_i \in W^{1,2}(\Omega);\ \mathbf{v}_i = 0 \text{ on } \Gamma_{in} \cup \Gamma_{wall}, i = 1, 2, 3\}\ \mathbf{v}_D = \mathbf{v}_m$ on Λ_{in} and $\mathbf{v}_D = 0$ on Λ_{wall}, $P = L^2(\Omega)$ such that for all $(\mathbf{u}, q) \in V \times P$

$$\int_\Omega \frac{\partial \mathbf{v}}{\partial t} \cdot \mathbf{u}\, \mathrm{d}x + \int_\Omega (\nabla \mathbf{v})\mathbf{v} \cdot \mathbf{u}\, \mathrm{d}x = \frac{1}{\varrho} \int_\Omega \mathbf{T} \colon \nabla \mathbf{u}\, \mathrm{d}x, \tag{14}$$

$$\int_\Omega q \operatorname{div} \mathbf{v}\, \mathrm{d}x = 0. \tag{15}$$

The discretization in time is done by an implicit one step difference method and with regard to spatial discretization, the function spaces V, P are approximated by standard piecewise polynomial spaces, i.e. Taylor–Hood P_2/P_1 elements.

The PPE and STE problems are cast in weak forms as follows:

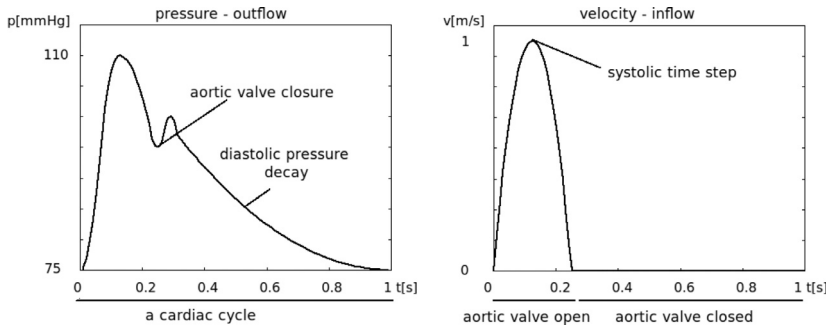

Fig. 1. Dependence of the prescribed outlet pressure and inlet velocity functions P and V on the time.

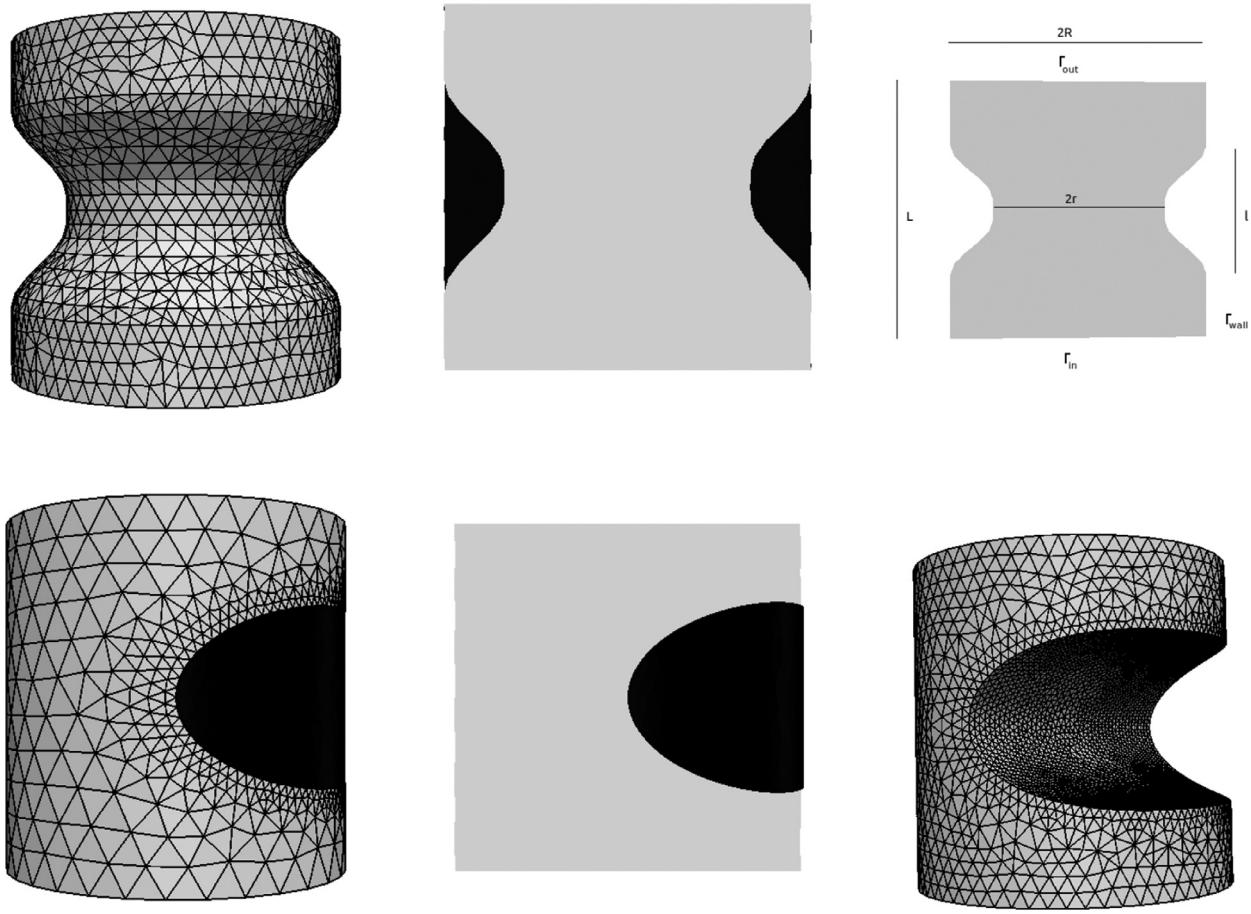

Fig. 2. The first row: three-dimensional mesh for reference flow representing the valve with the symmetric stenosis with 55% severity, for illustration the slices of the computational mesh are also displayed. Grey parts represent the domain of valve, black parts represent the tissue causing the stenosis. The second row: three-dimensional mesh for reference flow representing the valve with the 50% non-symmetric stenosis, the slice of a domain and another view to the mesh are provided. The sizes of the meshes: $L = 2.4$ cm, $l = 1.2$ cm, $R = 1.2$ cm, $r_{sym} = 0.805$ cm.

PPE: Find $(q_{\mathrm{ppe}}, r) \in P_P \times \mathcal{R}$ such that for all $(\widehat{q}, \widehat{r}) \in P_P \times \mathcal{R}$

$$\int_\Omega \nabla q_{\mathrm{ppe}} \cdot \nabla \widehat{q}\,\mathrm{d}x = \int_\Omega \mathbf{f} \cdot \nabla \widehat{q}\,\mathrm{d}x + \int_{\Gamma_{\mathrm{out}}} r\widehat{q}\,\mathrm{d}s,$$
$$\int_{\Gamma_{\mathrm{out}}} (q_{\mathrm{ppe}} - p)\widehat{r}\,\mathrm{d}s = 0. \qquad \text{(PPE)}$$

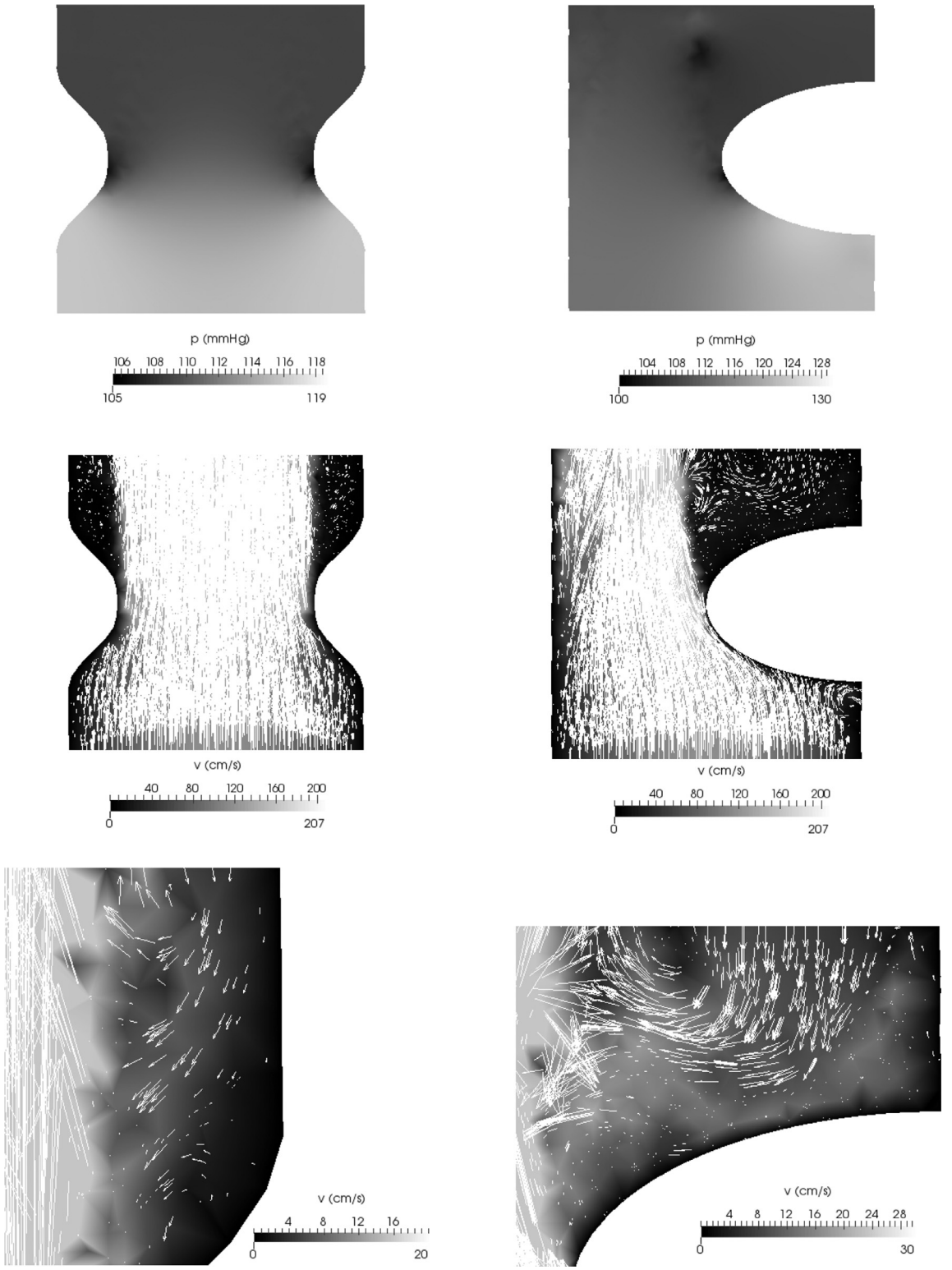

Fig. 3. The first two rows depict the distribution of the reference pressure p_{ref} and the reference velocity $\mathbf{v}_{\text{ref}}$ for symmetric (left column) and non-symmetric (right column) domains; the third row contains the detail of the velocity field $\mathbf{v}_{\text{ref}}$ on the slice near the outlet to show the regurgitation in flow.

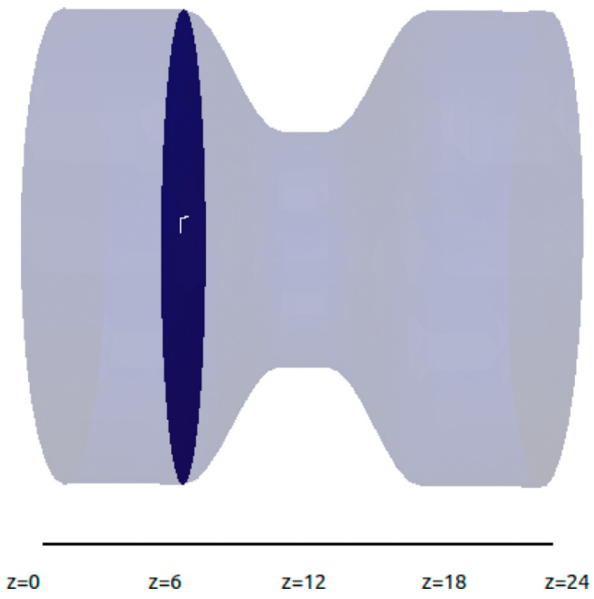

Fig. 4. Cross-section areas Γ along the centereline.

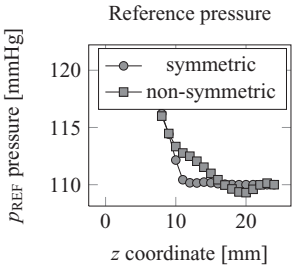

Fig. 5. The reference pressure p_{REF} (23) computed over the cross-sections as a function of the position along the centerline for two different geometries during a systolic time step.

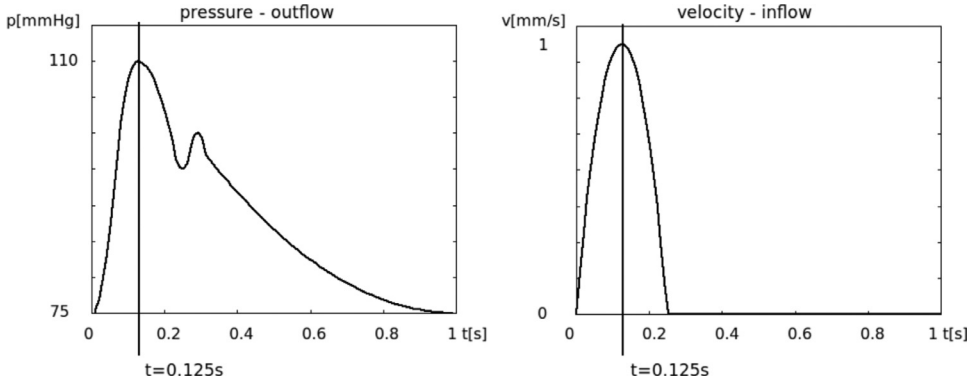

Fig. 6. Systolic time step $t = 0.125$ s for computations of PPE and STE methods.

STE: Find $(\mathbf{w}, q_{\mathrm{ste}}, r) \in V \times P_S \times \mathcal{R}$ such that for all $(\widehat{\mathbf{w}}, \widehat{q}, \widehat{r}) \in V \times P_S \times \mathcal{R}$

$$\int_\Omega \nabla \mathbf{w} \colon \nabla \widehat{\mathbf{w}} \mathrm{d}x - \int_\Omega q_{\mathrm{ste}} \operatorname{div} \widehat{\mathbf{w}} \mathrm{d}x = \int_\Omega \mathbf{f} \cdot \widehat{\mathbf{w}} \mathrm{d}x,$$

$$\int_{\Gamma_{\mathrm{out}}} r\widehat{q} \mathrm{d}s + \int_\Omega \widehat{q} \operatorname{div} \mathbf{w} \mathrm{d}x = 0$$

$$\int_{\Gamma_{\mathrm{out}}} (q_{\mathrm{ste}} - p)\widehat{r} \mathrm{d}s = 0. \tag{STE}$$

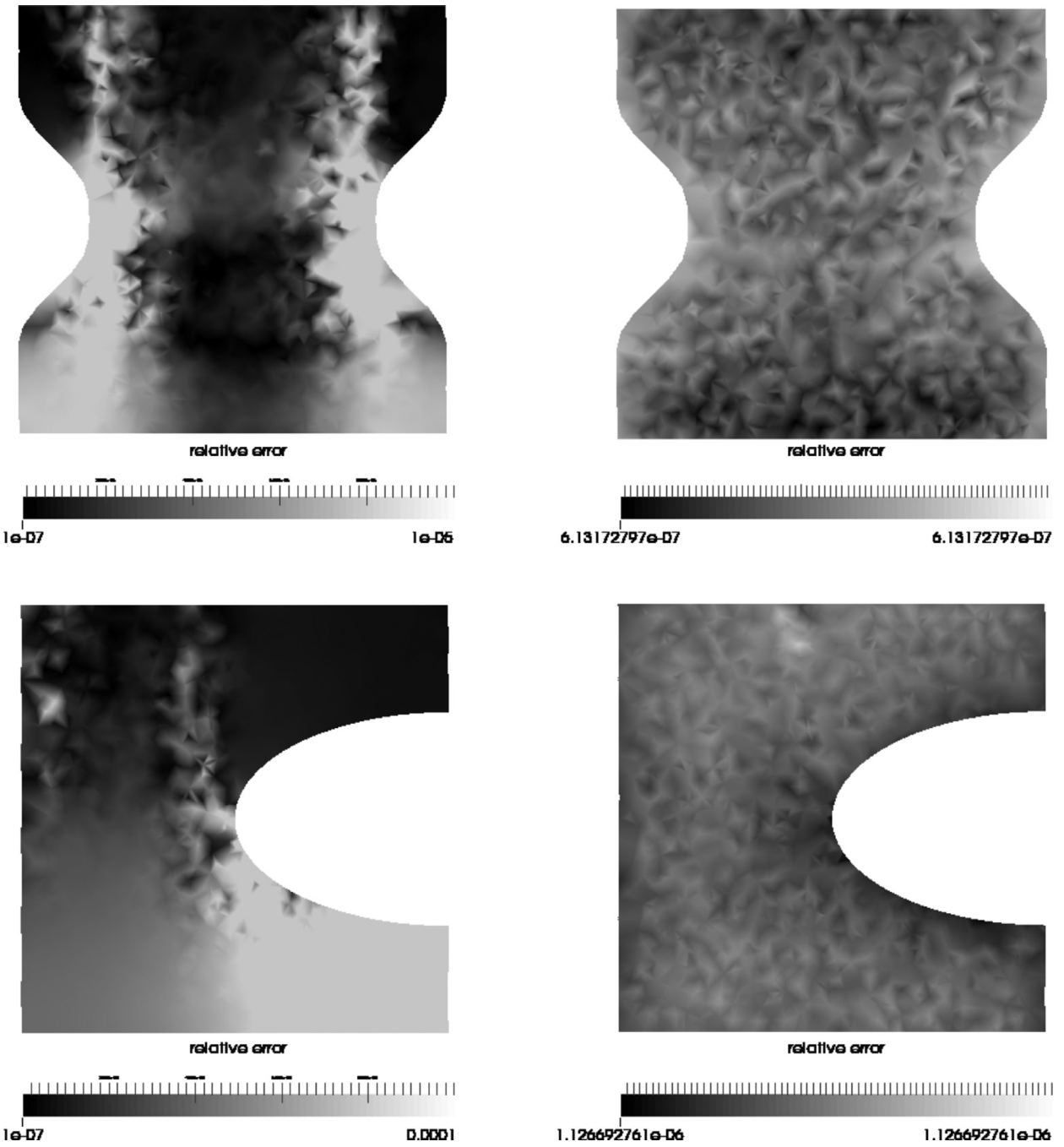

Fig. 7. Errors $|q_{\mathrm{ppe}} - p_{\mathrm{ref}}|$ (left column) and $|q_{\mathrm{ste}} - p_{\mathrm{ref}}|$ (right column) in mmHg on a slice of the domain.

Standard FEM discretization is used to find the approximate solution to these problems. The space P_S is approximated by piecewise P_1 functions and the spaces P_P and V by piecewise P_2 functions. The space $\mathcal{R}$ is a one dimensional space of constants on the computational domain and is used to enforce the additional condition on the mean value of the pressure over the Γ_{out} part of the boundary by means of a global Lagrange multiplier.

2. Numerical results

In Sections 1.1.1 and 1.1.2 we introduced two approaches to ascertain the pressure directly from the velocity field. In order to compute the results achieved by these two methods we introduce the reference velocity field $\mathbf{v}_{\mathrm{ref}}$ given as a numerical solution

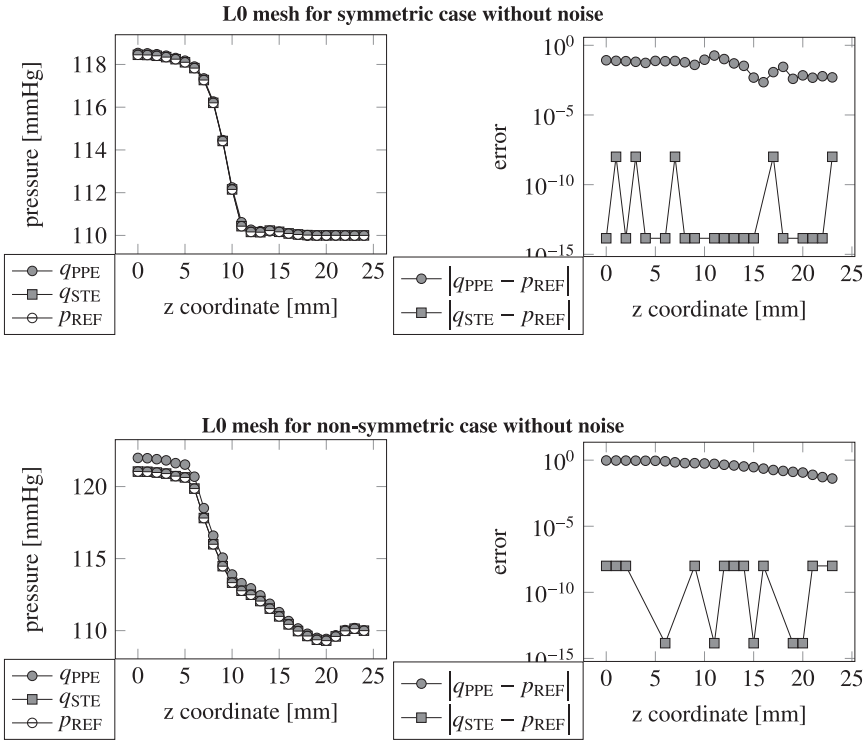

Fig. 8. Results on L0 mesh without noise. First column: The reference and obtained pressure computed through the formula (23). Second column: The absolute value of the difference between the reference and obtained pressure.

Table 2
Errors in the pressure drops for fine data.

	$\lvert p_{REF}^{drop} - q_{PPE}^{drop} \rvert$	$\lvert p_{REF}^{drop} - q_{STE}^{drop} \rvert$
Symmetric	8.42e−02	1.42e−14
Non-symmetric	9.44e−01	1.00e−08

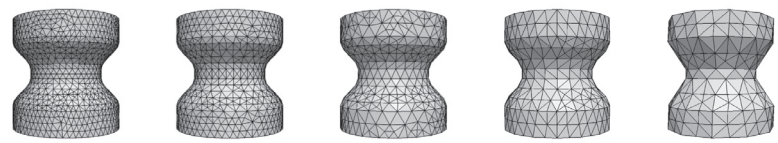

Fig. 9. The computational mesh L0 for the reference flow (16) and the coarser meshes for ascertaining pressure for the symmetric case.

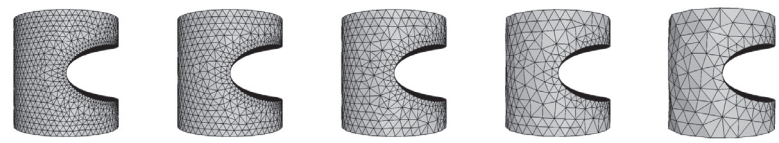

Fig. 10. The computational mesh L0 for the reference flow (16) and the coarser meshes for ascertaining the pressure for non-symmetric case.

Table 3
Relative errors for PPE and STE methods.

	Symmetric case			Non-symmetric case		
	$\frac{\lvert q_{\mathrm{PPE}}-p\rvert_{L^2}}{\lvert p\rvert_{L^2}}$	$\frac{\lvert q_{\mathrm{STE}}-p\rvert_{L^2}}{\lvert p\rvert_{L^2}}$	Ratio	$\frac{\lvert q_{\mathrm{PPE}}-p\rvert_{L^2}}{\lvert p\rvert_{L^2}}$	$\frac{\lvert q_{\mathrm{STE}}-p\rvert_{L^2}}{\lvert p\rvert_{L^2}}$	Ratio
L0N0	6.40362e−04	1.49962e−14	–	3.49798e−03	1.15522e−14	–
L1N0	1.48584e−03	1.03299e−03	1.438	2.53496e−03	1.67932e−03	1.510
L2N0	2.24117e−03	1.45550e−03	1.540	3.32938e−03	2.19963e−03	1.514
L3N0	6.52214e−03	2.14646e−03	3.039	5.81674e−03	3.05025e−03	1.907
L4N0	9.37379e−03	3.13883e−03	2.986	8.45922e−03	4.04690e−03	2.090
L0N5	9.03476e−04	6.66165e−04	1.356	4.91294e−03	2.80946e−03	1.749
L1N5	1.81613e−03	1.25684e−03	1.445	4.94317e−03	3.33793e−03	1.481
L2N5	2.40288e−03	1.52389e−03	1.577	4.84234e−03	3.82561e−03	1.266
L3N5	7.10268e−03	2.49039e−03	2.852	8.07420e−03	6.46264e−03	1.249
L4N5	9.14510e−03	3.17592e−03	2.880	9.87244e−03	8.45561e−03	1.168
L0N10	1.45388e−03	1.32869e−03	1.094	6.89162e−03	5.62814e−03	1.224
L1N10	2.37458e−03	1.74884e−03	1.358	8.12804e−03	6.08856e−03	1.335
L2N10	2.86221e−03	1.83955e−03	1.556	7.75631e−03	6.69936e−03	1.158
L3N10	7.81501e−03	3.12834e−03	2.498	1.19152e−02	1.20042e−02	0.993
L4N10	9.06467e−03	3.44484e−03	2.631	1.55605e−02	1.57420e−02	0.988

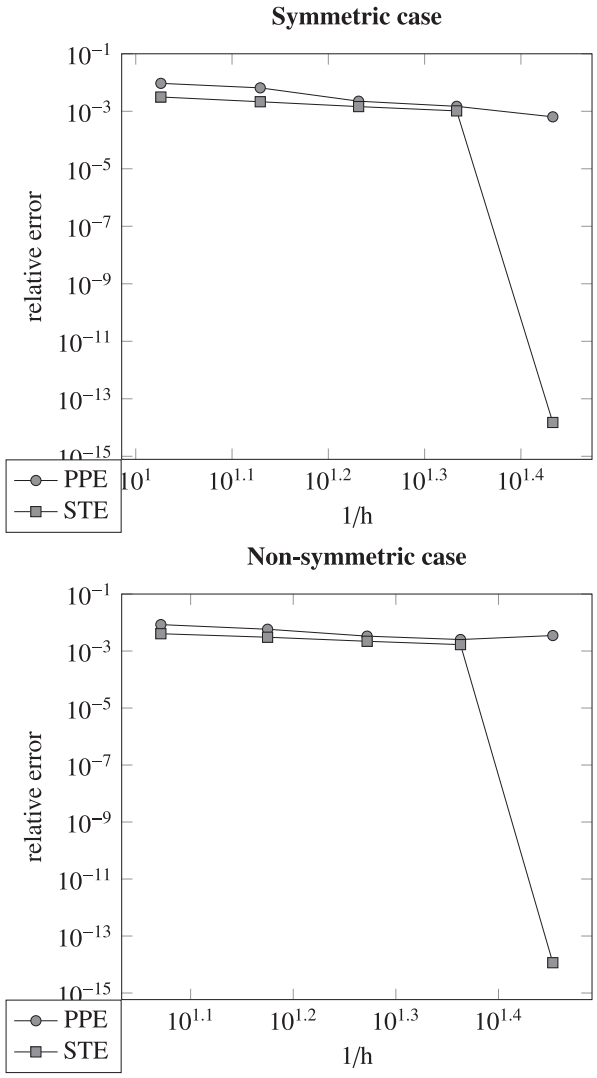

Fig. 11. Convergence curves of relative errors for coarse data without noise.

Table 4
Error in the pressure drop for PPE and STE methods.

	Symmetric case			Non-symmetric case		
	$\lvert p_{REF}^{drop} - q_{PPE}^{drop} \rvert$	$\lvert p_{REF}^{drop} - q_{STE}^{drop} \rvert$	Ratio	$\lvert p_{REF}^{drop} - q_{PPE}^{drop} \rvert$	$\lvert p_{REF}^{drop} - q_{STE}^{drop} \rvert$	Ratio
L0N0	0.08418611	0.00000000	–	0.94382822	0.00000001	–
L1N0	0.23119261	0.04775308	4.841	0.44089585	0.11688687	3.772
L2N0	0.32041433	0.04229078	7.576	0.50084404	0.09621437	5.206
L3N0	1.19112938	0.13581371	8.770	1.00590735	0.03276853	30.697
L4N0	1.86391129	0.26864459	6.938	1.41908330	0.14511580	9.779
L0N5	0.04192082	0.10039530	0.418	1.16712177	0.29000982	4.024
L1N5	0.33371535	0.06318706	5.281	0.99928618	0.17859268	5.595
L2N5	0.23331512	0.13818813	1.688	0.71064417	0.01646946	43.149
L3N5	1.35402752	0.27655645	4.896	1.63957690	1.18700155	1.381
L4N5	1.89644339	0.35499218	5.342	0.21993680	1.43692624	0.153
L0N10	0.00337416	0.19589881	0.017	1.39336416	0.58381577	2.387
L1N10	0.43341550	0.16972165	2.554	1.55473599	0.46915924	3.314
L2N10	0.14353863	0.23876727	0.601	0.91691954	0.05801561	15.805
L3N10	1.51290953	0.41190733	3.673	2.27005748	2.40155599	0.945
L4N10	1.92480230	0.43722139	4.402	1.86438319	3.02559840	0.616

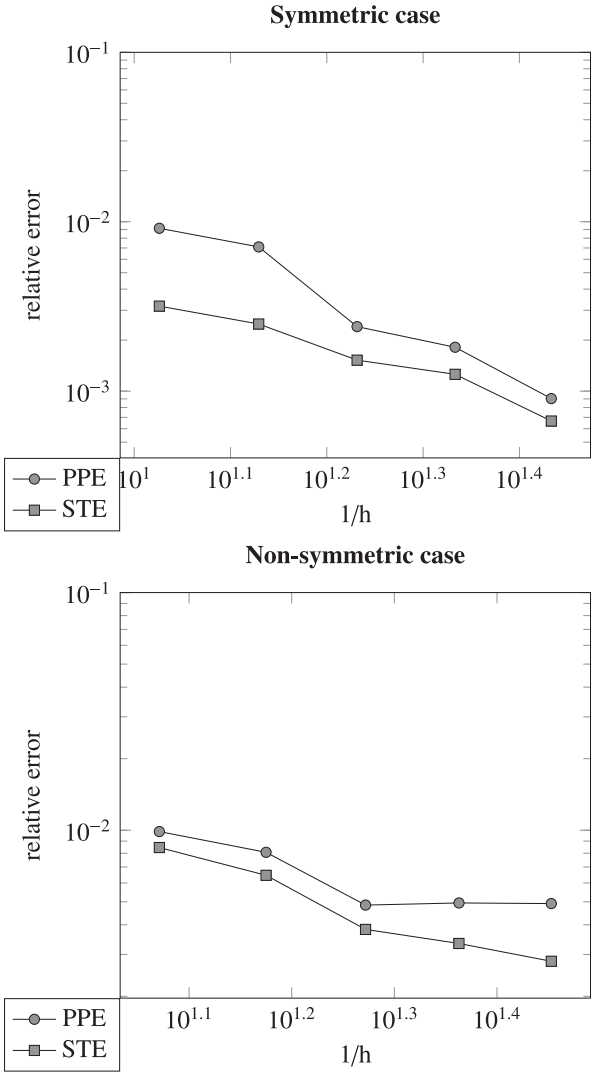

Fig. 12. Convergence curves of relative errors for coarse data with 5% noise.

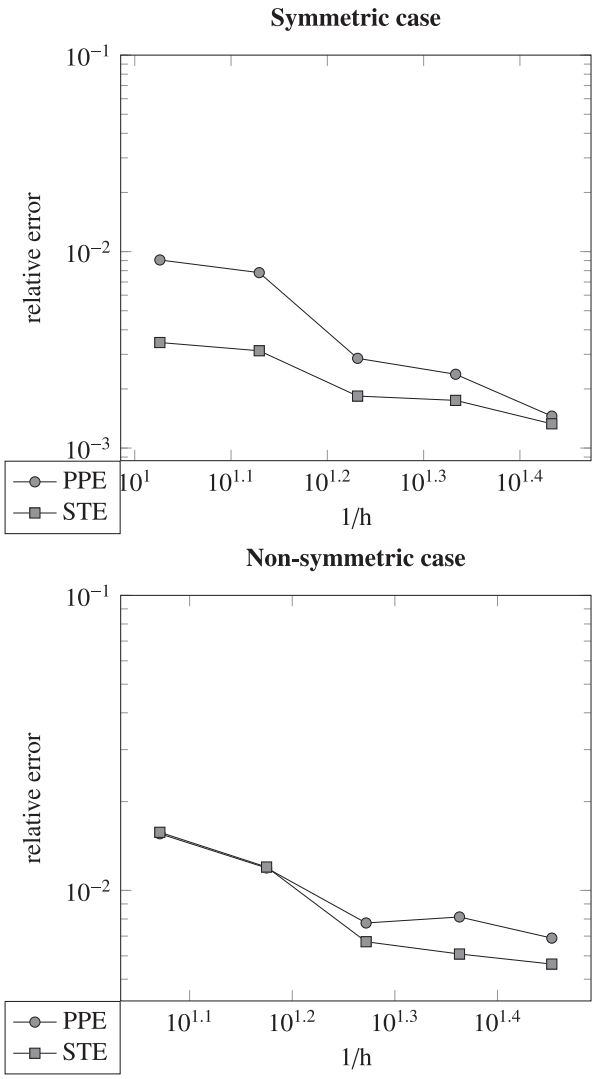

Fig. 13. Convergence curves of relative errors for coarse data with 10% noise.

of the incompressible Navier–Stokes equations. This velocity field $\mathbf{v}_{\text{ref}}$ will serve as the input data for PPE and STE methods, and we refer to $\mathbf{v}_{\text{ref}}$ as the reference flow. The computed pressure p_{ref} will be used as the reference pressure used to compare the accuracy of these two methods.

2.1. Reference flow

In a given domain $\Omega \subset \mathbf{R}^3$, representing the simplified aortic valve, the velocity $\mathbf{v}_{\text{ref}}$ and pressure p_{ref} satisfy

$$\frac{\partial \mathbf{v}_{\text{ref}}}{\partial t} + (\nabla \mathbf{v}_{\text{ref}})\mathbf{v}_{\text{ref}} + \nabla \frac{p_{\text{ref}}}{\varrho} - \operatorname{div}(2\nu \mathbf{D}(\mathbf{v}_{\text{ref}})) = \mathbf{0}, \tag{16}$$

$$\operatorname{div} \mathbf{v}_{\text{ref}} = 0, \tag{17}$$

with the boundary conditions

$$\mathbf{v}_{\text{ref}} = \mathbf{0} \quad \text{on } \Gamma_{\text{wall}}, \tag{18}$$

$$\mathbf{v}_{\text{ref}} = \mathbf{v}_{\text{in}} \quad \text{on } \Gamma_{\text{in}}, \tag{19}$$

$$\mathbf{T}\mathbf{n} - \frac{1}{2}\varrho(\mathbf{v}_{\text{ref}} \cdot \mathbf{n})_{-}\mathbf{v}_{\text{ref}} = -P(t)\mathbf{n} \quad \text{on } \Gamma_{\text{out}}, \tag{20}$$

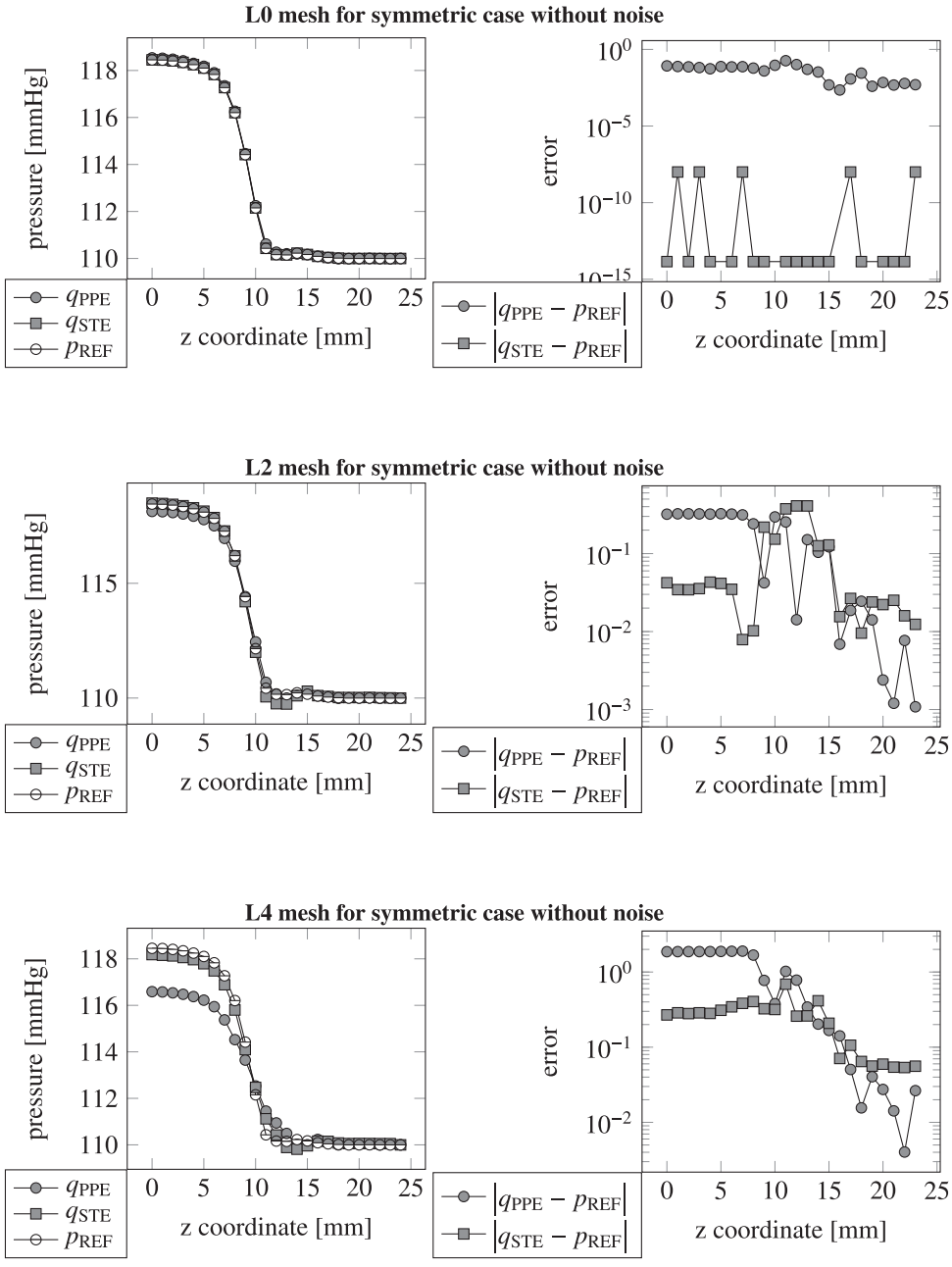

Fig. 14. Reference and obtained pressures computed through the formula (23) in the first column and the absolute value of difference between the reference and obtained pressures in a second column for both methods.

where $\mathbf{T} = -p\mathbf{I} + 2\mu\mathbf{D}(\mathbf{v}_{\text{ref}})$. The vector $\mathbf{n}$ is the unit normal vector to the boundary $\partial\Omega$ which consists of three parts: Γ_{wall} denotes the walls and Γ_{in}, Γ_{out} are the inlet and outlet, respectively. The dynamic viscosity is taken as a constant $\mu = 3.7 \times 10^{-3}$ kg/ms, density $\varrho = 1000\,\text{kg/m}^3$, kinematic viscosity $\nu = \frac{\mu}{\varrho}$. At the outlet we prescribe the mean value $P(t)$ of the pressure which is supposed to be based on information from measurements in the aorta as a function of time. In stenotic valves, regurgitation occurs and it can lead to instabilities. The backflow stabilization used at the outlet is studied in Braack and Mucha (2014) and Bertoglio and Caiazzo (2014). The velocity v_{in} is given as a parabolic profile with its magnitude scaled by a time dependent factor $V(t)$, i.e.

$$v_{\text{in}}(t, \mathbf{x}) = 1.5V(t)\max(|\mathbf{x} - \mathcal{T}|^2, 0)/r^2, \tag{21}$$

where $\mathcal{T}$ is the centerpoint of an input plane and r is its radius for the parabolic profile.

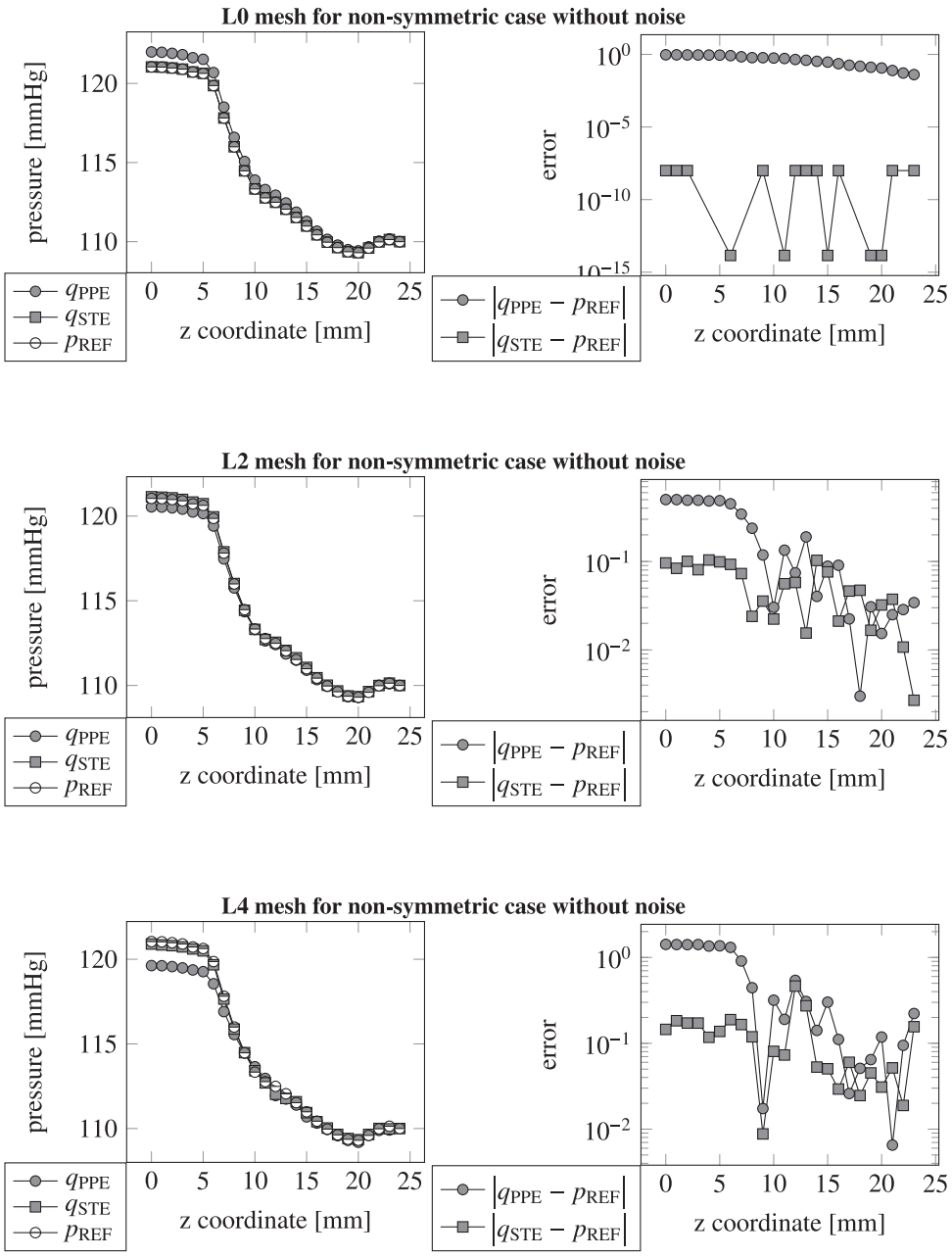

Fig. 15. Reference and obtained pressures computed through the formula (23) in the first column and the absolute value of difference between the reference and obtained pressures in a second column for both methods.

Both functions $P(t)$ and $V(t)$ depend on the stenosis severity. For the purpose of this work, we used the functions $P(t)$ and $V(t)$ with the peak velocity $v_{max} = 1.0$ m/s, the peak pressure $p_{max} = 110$ mmHg and the diastolic pressure $p_{min} = 75$ mmHg, see Fig. 1. For better illustration we use a unit millimeter of mercury while 1 Pa = 0.0075 mmHg. One cardiac cycle lasts 1 s, the time when the aortic valve is considered open is 0.25 s. The detailed description of the terms shown in Fig. 1 will be provided in Part 2 of this study.

The computational meshes for the reference flow are shown in Fig. 2. The first one represents an aortic valve with 55% symmetric severity where the severity is given by formula (22) as a relation between the area of the healthy part, approximated here by a circle with radius R, and the area of the stenotic part, approximated by a circle with radius r, i.e.

$$\text{severity} = \left(1 - \frac{\text{area}_r}{\text{area}_R}\right) \times 100\% \tag{22}$$

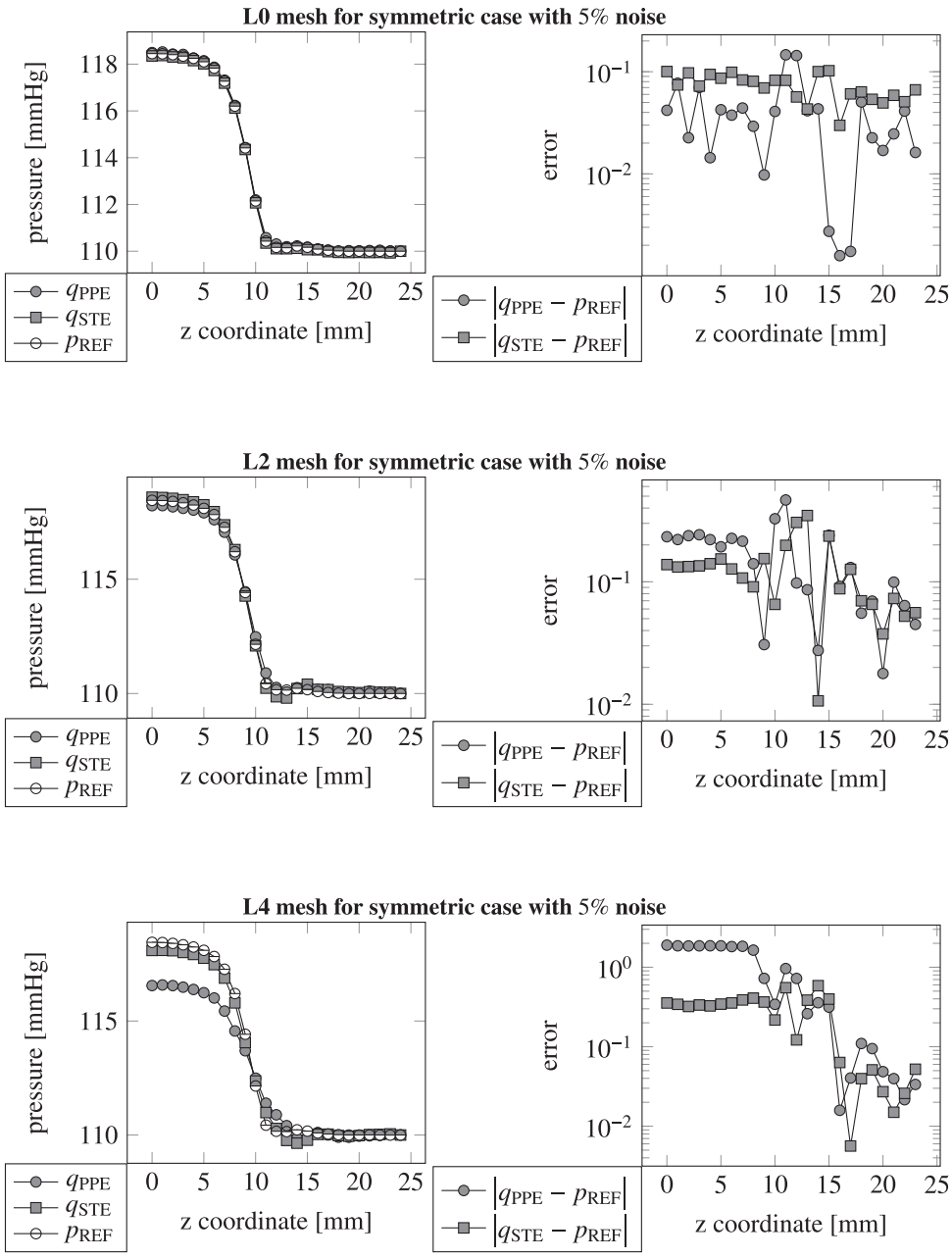

Fig. 16. Reference and obtained pressures computed through the formula (23) in the first column, and the absolute value of difference between the reference and obtained pressures in the second column, for both methods.

The length of the valve $L = 2.4$ cm and the radius of the healthy part $R = 1.2$ cm. For the stenotic part the length $l = 1.2$ cm and the radius $r = 0.805$ cm. The second mesh with the same L, l and R represents an aortic valve with 50% non-symmetric severity.

The resulting reference pressure p_{ref} and velocity field $\mathbf{v}_{\text{ref}}$ are shown on the slice of the mesh in Fig. 3. The maximal local Reynolds numbers $\text{Re} = \frac{UL}{\nu}$ for these two problems, in symmetric and nonsymmetric domains, with characteristic length L = 1 mm, kinematic viscosity $\nu = 3{:}\,71\ (\text{mm})^2\,\text{s}^{-1}$ and characteristic velocities of U = 2077 (mm) s^{-1} and U = 2838 (mm) s^{-1}, are 560 and 765, respectively.

In the next section, we will compare the pressures q_{ppe} and q_{ste} obtained by the two methods proposed in Sections 1.1.1 and 1.1.2 with this reference pressure p_{ref}. To do that, we will compute the pressure as an integral over the slices along the centerline, see Eq. (23). The centerline is an axis passing through the vessel, Γ denotes the cross-sectional area along the centerline, see Fig. 4. The resulting curves presenting the pressure drop within the domain, computed through the formula (23), are shown in

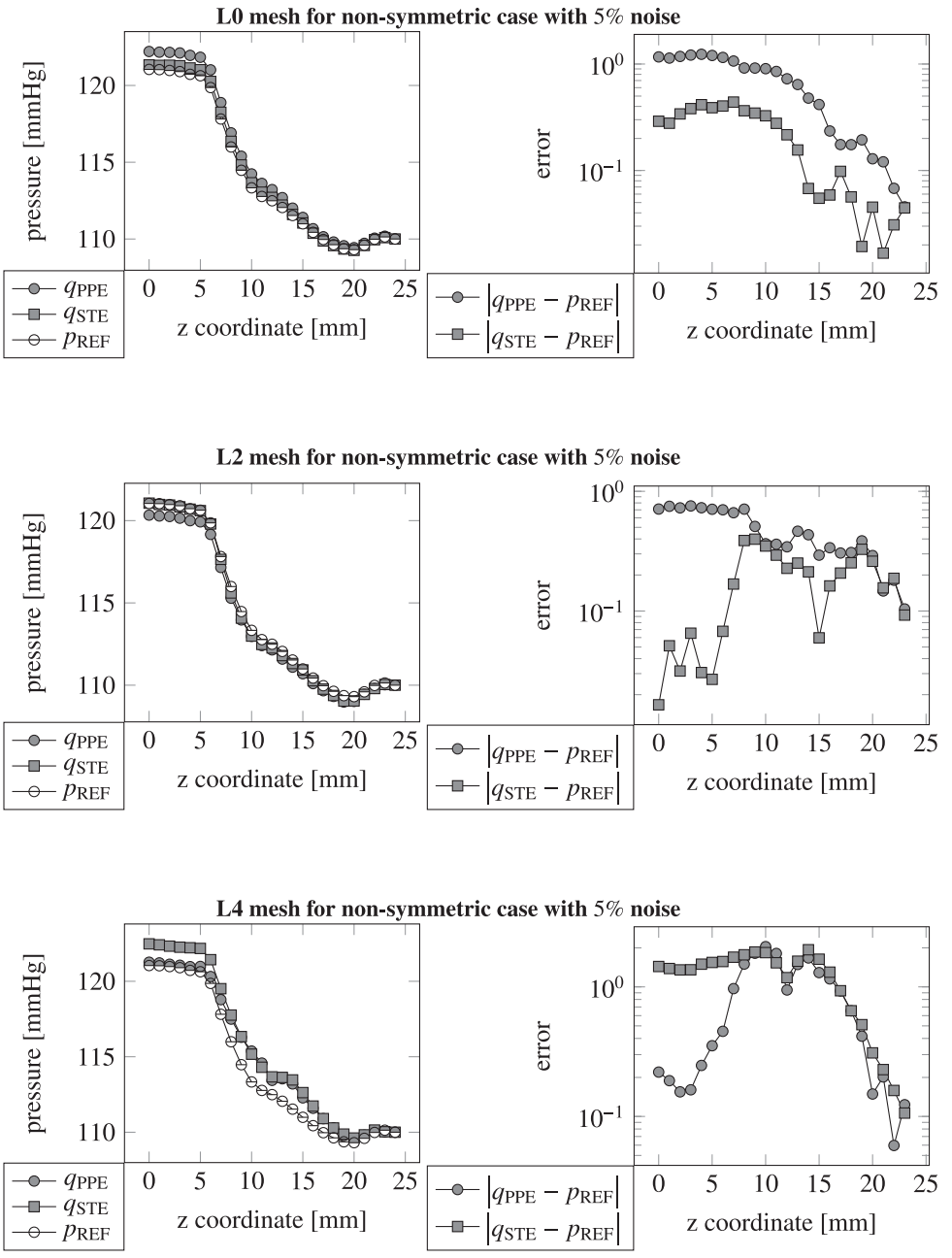

Fig. 17. Reference and obtained pressures computed through the formula (23) in the first column, and the absolute value of difference between the reference and obtained pressures in a second column, for both methods.

the Fig. 5. The centerline here passes through the z axis so we will use the term "z coordinate" for the figures, not "cross-section area along the centerline".

$$p_{REF} = \frac{\int_\Gamma p_{ref}\, dS}{\text{area}(\Gamma)} \tag{23}$$

We define similarly q_{PPE} and q_{STE} for q_{ppe} and q_{ste} respectively. While we will ascertain pressure only in a systolic time step $t = 0.125$ s and at that time we compute p_{REF}, q_{PPE} and q_{STE} as a function of the z coordinate.

2.2. Comparison of the methods with regard to the ascertainment of the pressure

In this section we will compare the results for each of the methods introduced in Sections 1.1.1 and 1.1.2 with respect to the quality of the input velocity field. All the tests will be computed in a systolic time step $t = 0.125$ s see. Fig. 6.

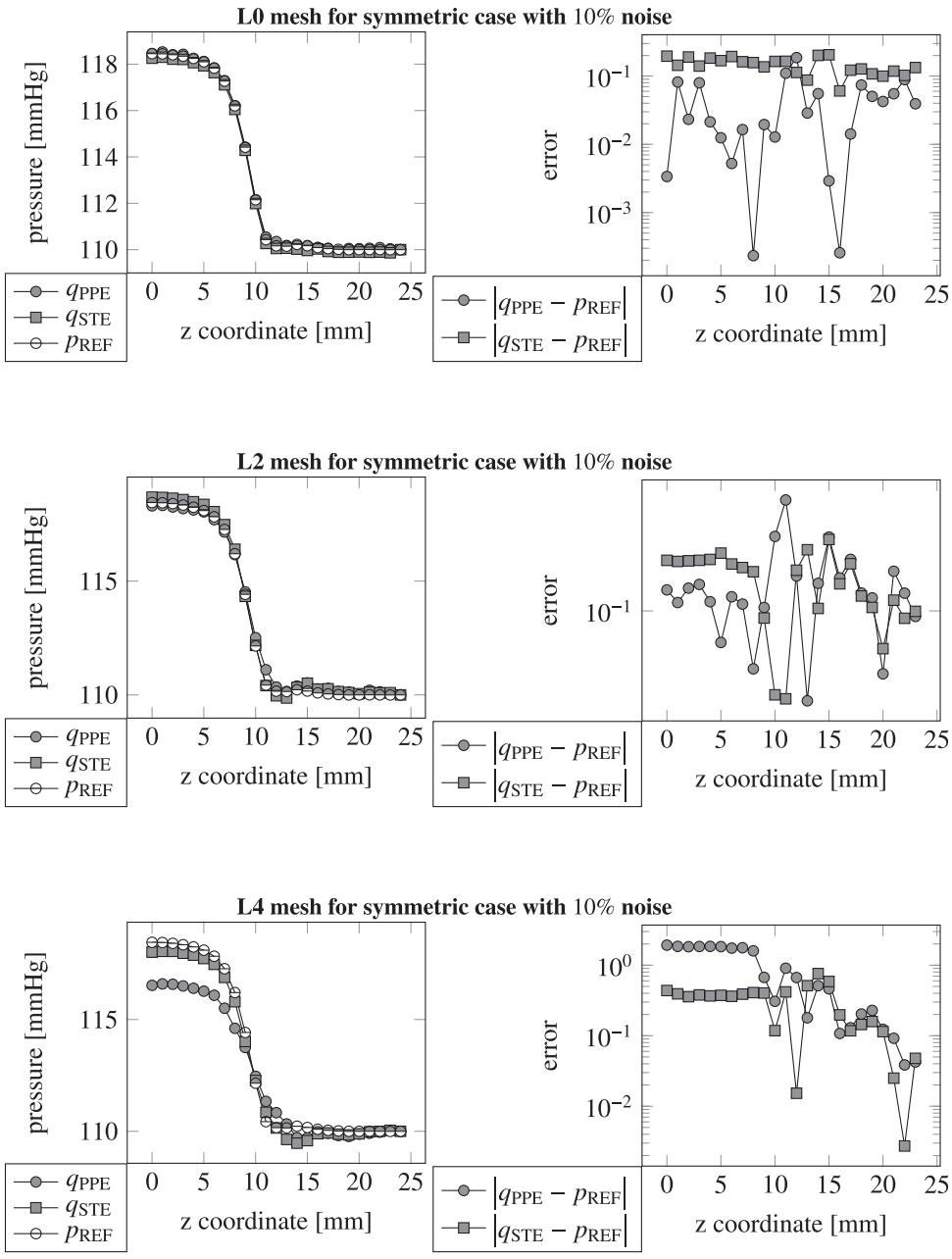

Fig. 18. Reference and obtained pressures computed through the formula (23) in the first column, and the absolute value of difference between the reference and obtained pressures in a second column, for both methods.

2.2.1. Fine data

We will start with velocity field given on the same very fine mesh as that for which we know the velocity field exactly, i.e. velocity field known at every vertex of the mesh and with the velocity field measured exactly without noise. This case corresponds to the computation on L0 mesh, see Figs. 9 and 10.

For both cases, symmetric and non-symmetric, we compute the relative error $\frac{\|q_{ppe}-p_{ref}\|_{L^2}}{\|p_{ref}\|_{L^2}}$ and $\frac{\|q_{ste}-p_{ref}\|_{L^2}}{\|p_{ref}\|_{L^2}}$ where the obtained pressures q_{ppe} and q_{ste} were linearly interpolated to the finer mesh where p_{ref} was computed. The relative errors are shown in Table 1 and the point-wise errors are plotted in Fig. 7.

While we are fixing the outlet the pressures $p_{REF} = q_{PPE} = q_{STE}$, computed through the formula (23), we are interested in the comparison of the pressure drops $q^{drop}_{PPE} := q_{PPE}(\text{inlet}) - q_{PPE}(\text{outlet})$ and $q^{drop}_{STE} := q_{STE}(\text{inlet}) - q_{STE}(\text{outlet})$ compared to the reference pressure drop $p^{drop}_{REF} := p_{REF}(\text{inlet}) - p_{REF}(\text{outlet})$.

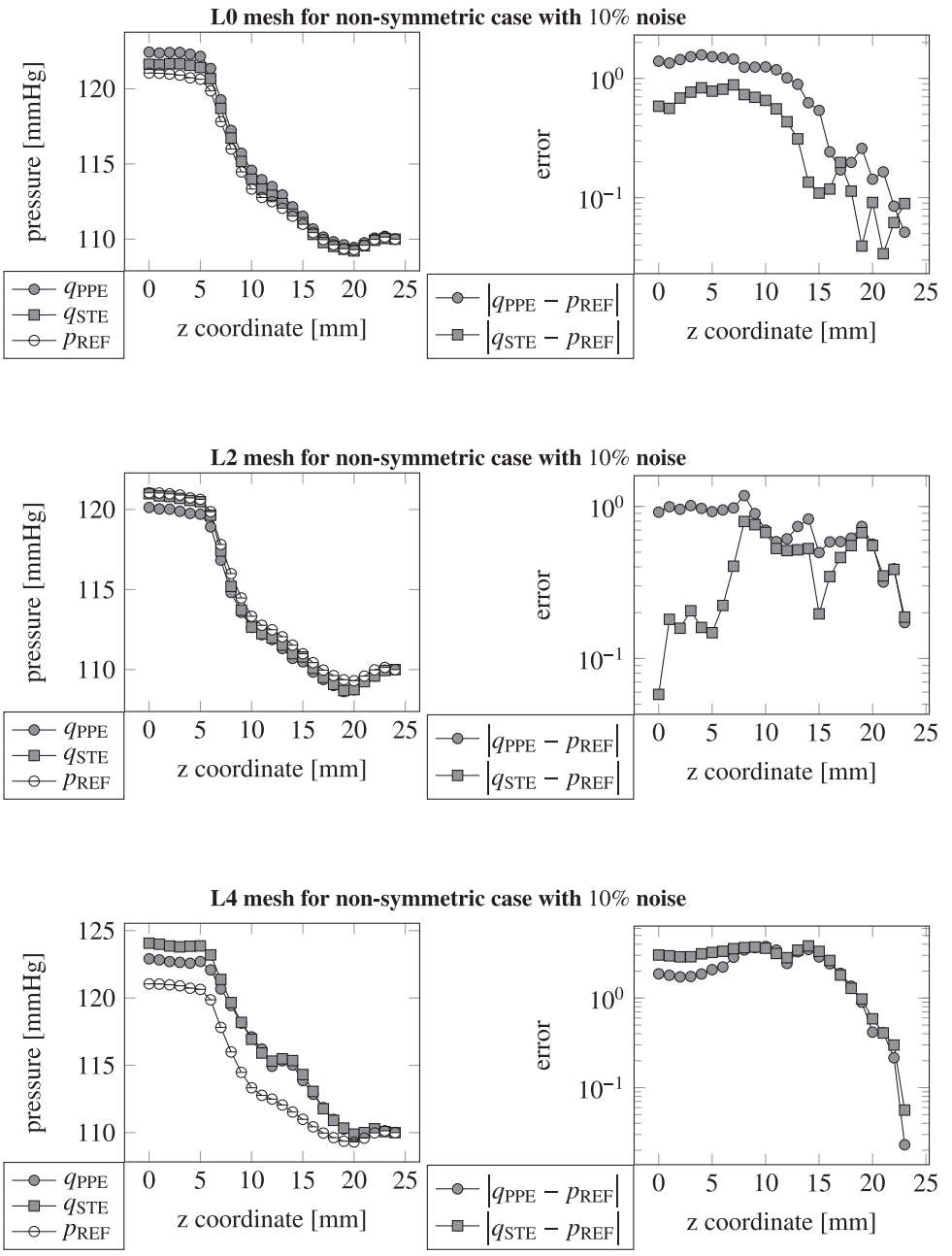

Fig. 19. Reference and obtained pressures computed through the formula (23) in the first column, and the absolute value of difference between the reference and obtained pressures in a second column, for both methods.

The pressures p_{REF}, q_{PPE} and q_{STE} are shown in the Fig. 8 and the differences between the q_{PPE}^{drop} and q_{STE}^{drop} in comparison with p_{REF}^{drop} are shown in Table 2.

2.2.2. Coarse data

Next, we will carry out more tests with less accurate velocity fields with fewer points where we pretend to know the velocity exactly. This means computations on coarser meshes. All of these meshes, referred to here as level L0 for the finest mesh and L4 for the coarsest mesh, are shown in Figs. 9 and 10.

We also compute the relative errors $\frac{\|q_{ppe}-p_{ref}\|_{L^2}}{\|p_{ref}\|_{L^2}}$ and $\frac{\|q_{ste}-p_{ref}\|_{L^2}}{\|p_{ref}\|_{L^2}}$ for these five types of meshes. The results are shown in Table 3, the convergence curves for symmetric and non-symmetric case are shown in Fig. 11. $1/h$ here is taken as cube root of the number of nodes of the mesh.

Pressures p_{REF}, q_{PPE} and q_{STE} and also the errors $|q_{\mathrm{PPE}} - p_{\mathrm{REF}}|$ are plotted in Fig. 14–19. The errors in the pressure drop estimations are shown in Table 4.

2.2.3. Data with the noise

In this section we want to simulate the fact that velocity is measured with error or noise. While there is an interpolation error due to the limited amount of points where we know the velocity, we will also include the error of the measurement which can be as much as 5% or 10%. This means that the velocity $\mathbf{v}_{\mathrm{ref}}(\overline{\mathbf{x}})$ at the point $\overline{\mathbf{x}}$ is replaced by the $\mathbf{v}_{\mathrm{meas}}(\overline{\mathbf{x}}) = (1 \pm \varepsilon(\overline{\mathbf{x}}))\mathbf{v}_{\mathrm{ref}}(\overline{\mathbf{x}})$ where $\varepsilon(\overline{\mathbf{x}}) \in [0, 0.05]$ for maximal 5% error, $\varepsilon(\overline{\mathbf{x}}) \in [0, 0.1]$ for maximal 10% error respectively. That is the vector of the reference (exact) velocity is (due to the measurement) lessened or increased in magnitude by the error 5% or 10%. This is numerically simulated by adding a random number $\varepsilon \in [-0.05, 0.05]$, $\varepsilon \in [-0.1, 0.1]$ respectively, to each point where we know the velocity.

We can combine these two problems (error due to information at a limited amount of points and error due to the deviations of measured and exact vectors). We will distinguish the meshes for computation, see Figs. 9 and 10, as levels L0–L4 and the error due to the deviation as N0, N5 and N10 for including noise 0%, 5% or 10%.

The relative errors between the reference and obtained pressure $\frac{\|q_{\mathrm{ppe}} - p_{\mathrm{ref}}\|_{L^2}}{\|p_{\mathrm{ref}}\|_{L^2}}$ and $\frac{\|q_{\mathrm{ste}} - p_{\mathrm{ref}}\|_{L^2}}{\|p_{\mathrm{ref}}\|_{L^2}}$ are shown for both geometries (symmetric and non-symmetric) and for all computational meshes L0–L4 in Table 3. They are also shown in Figs. 12 and 13. $1/h$ here is taken as the cube root of the number of nodes of the mesh.

Pressures p_{REF}, q_{PPE} and q_{STE} and also the errors $|q_{\mathrm{PPE}} - p_{\mathrm{REF}}|$ are plotted in Fig. 14–19. The errors in pressure drop estimations are shown in Table 4.

The reference pressure for the symmetric and non-symmetric problems is shown in Fig. 5, the obtained pressures for different problems are shown in Fig. 14–19.

3. Discussion

In this study, we have developed a mathematically rigorous methodology for the determination of the pressure field from a knowledge of the velocity field in the case of the Navier–Stokes fluid, with a view toward the determination of the pressure loss across a diseased valve. In Part 1 we tested the problem for idealized geometries. The study captures some of the salient features concerning the flow of blood in cardiovascular systems, such as the mechanical properties of blood and the spatiotemporal characteristics of ventricular, trans-valvular, and arterial blood flow.

Also, we incorporated the normal physiological mechanical properties of the fluid. However, fully integrating the deformable conduit with moving fluid/solid boundary into the existing model, in order to develop a comprehensive mathematical model, is considerably more difficult and will be the focus of future endeavors. Testing a more refined model against clinically relevant datasets then may be undertaken.

Acknowledgments

J. Hron Malek and H. Švihlová were supported by KONTAKT II (LH14054) financed by MŠMT ČR. K. R. Rajagopal thanks the National Science Foundation, United States for its support.

References

Akins, C. W., Travis, B., & Yoganathan, A. P. (2008). Energy loss for evaluating heart valve performance. *The Journal of Thoracic and Cardiovascular Surgery, 136*(4), 820–833.

Bertoglio, C., & Caiazzo, A. (2014). A tangential regularization method for backflow stabilization in hemodynamics. *Journal of Computational Physics, 261*, 162–171.

Bolin, C. D., & Raguin, L. G. (2008). Methodology to estimate the relative pressure field from noisy experimental velocity data. *Journal of Physics: Conference Series, 135*, 012020.

Braack, M., & Mucha, P. B. (2014). Directional do-nothing condition for the Navier-Stokes equations. *Journal of Computational Mathematics, 32*(5), 507–521.

Cayco, M. E., & Nicolaides, R. A. (1986). Finite element technique for optimal pressure recovery from stream function formulation of viscous flows. *Mathematics of Computation, 46*(174), 371.

Charonko, J. J., King, C. V., Smith, B. L., & Vlachos, P. P. (2010). Assessment of pressure field calculations from particle image velocimetry measurements. *Measurement Science and Technology, 21*, 105401.

Dabiri, J. O., Bose, S., Gemmell, B. J., Colin, S. P., & Costello, J. H. (2014). An algorithm to estimate unsteady and quasi-steady pressure fields from velocity field measurements. *The Journal of Experimental Biology, 217*(3), 331–336.

Dasi, L. P., Simon, H. A., Sucosky, P., & Yoganathan, A. P. (2009). Fluid mechanics of artificial heart valves. *Clinical and Experimental Pharmacology and Physiology, 36*(2), 225–237.

Guermond, J. L., Minev, P., & Shen, J. (2006). An overview of projection methods for incompressible flows. *Computer Methods in Applied Mechanics and Engineering, 195*(44–47), 6011–6045.

Gurka, R., Liberzon, A., Hefetz, D., & Rubinstein, D. (1999). Computation of pressure distribution using PIV velocity data. In *Proceedings of the 3rd international workshop on particle image velocimetry—PIV'99*.

Heys, J. J., Manteuffel, T. A., McCormick, S. F., Milano, M., Westerdale, J., & Belohlavek, M. (2010). Weighted least-squares finite elements based on particle imaging velocimetry data. *Journal of Computational Physics, 229*(1), 107–118.

Hron, J., & Madlik, M. (2007). Fluid-structure interaction with applications in biomechanics. *Nonlinear Analysis: Real World Applications, 8*(5), 1431–1458.

Krittian, S. B. S., Lamata, P., Michler, C., Nordsletten, D. A., Bock, J., Bradley, C. P., et al. (2012). A finite-element approach to the direct computation of relative cardiovascular pressure from time-resolved MR velocity data. *Medical Image Analysis, 16*, 1029–1037.

Liu, J.-G., Liu, J., & Pego, R. L. (2010). Stable and accurate pressure approximation for unsteady incompressible viscous flow. *Journal of Computational Physics, 229*(9), 3428–3453.

Logg, A., Mardal, K. A., & Wells, G. N. (Eds.). (2012). *Automated solution of differential equations by the finite element method: Vol. 84. Lecture Notes in Computational Science and Engineering*. Berlin/Heidelberg: Springer.

Maria Denaro, F. (2003). On the application of the Helmholtz-Hodge decomposition in projection methods for incompressible flows with general boundary conditions. *International Journal for Numerical Methods in Fluids, 43*(1), 43–69.
Prohl, A. (2008). On pressure approximation via projection methods for nonstationary incompressible Navier-Stokes equations. *SIAM Journal of Numerical Analysis, 47*(1), 158–180.
Rajagopal, K. R. (2015). Remarks on the notion of "pressure". *International journal of non-linear mechanics, 71*, 165–172.
Razzaq, M., Damanik, H., Hron, J., Ouazzi, A., & Turek, S. (2012). FEM multigrid techniques for fluid–structure interaction with application to hemodynamics. *Applied Numerical Mathematics, 62*(9), 1156–1170.
Shirokoff, D., & Rosales, R. R. (2011). An efficient method for the incompressible Navier–Stokes equations on irregular domains with no-slip boundary conditions, high order up to the boundary. *Journal of Computational Physics, 230*(23), 8619–8646.
Song, S. M., Leahy, R. M., Boyd, D. P., Brundage, B. H., & Napel, S. (1994). Determining cardiac velocity fields and intraventricular pressure distribution from a sequence of ultrafast CT cardiac images. *IEEE Transactions on Medical Imaging, 13*(2), 386–397.
Van Oudheusden, B. W. (2013). PIV-based pressure measurement. *Measurement Science and Technology, 24*(3), 032001.
Yang, G.-Z., Kilner, P. J., Wood, N. B., Underwood, S. R., & Firmin, D. N. (1996). Computation of flow pressure fields from magnetic resonance velocity mapping. *Magnetic Resonance in Medicine, 36*(4), 520–526.